



## Calhoun: The NPS Institutional Archive

---

Faculty and Researcher Publications

Faculty and Researcher Publications Collection

---

1985-09-01

# Dependence of atom ejection on electronic energy loss

Jakas, Mario M.

American Physical Society

---

Physical Review B, v. 32, no. 5, September 1, 1985, pp. 2752-2760

<http://hdl.handle.net/10945/47483>



Calhoun is a project of the Dudley Knox Library at NPS, furthering the precepts and goals of open government and government transparency. All information contained herein has been approved for release by the NPS Public Affairs Officer.

**Dudley Knox Library / Naval Postgraduate School**  
**411 Dyer Road / 1 University Circle**  
**Monterey, California USA 93943**

<http://www.nps.edu/library>

## Dependence of atom ejection on electronic energy loss

Mario M. Jakas\* and Don E. Harrison, Jr.

Naval Postgraduate School, Monterey, California 93943

(Received 3 January 1985)

This paper extends previous theoretical models to emphasize the influence of electronic energy losses upon the ejection of atoms by bombarding ions. This sensitivity of the sputtering yield to inelastic energy losses was first observed in computer simulations of sputtering. The theoretical analysis supports the simulation-derived conclusion that the total yield is much more sensitive to electronic energy losses by the *atoms* than to electronic energy losses of the bombarding ions, even when the ion is much lighter than the target atoms.

### I. INTRODUCTION

Although the ejection of atoms from metallic surfaces by bombarding energetic particles has been studied in detail both experimentally and theoretically, relatively less attention has been paid to the role of energy losses to electronic processes, so-called "inelastic energy losses" in the atom-ejection process.<sup>1-7</sup> To some extent, there is justification for the assumption that inelastic losses can be ignored, so most studies done in this field simply avoid dealing with the problem.

The transport theory of sputtering,<sup>1</sup> in which the sputtering yield is expressed as

$$Y = (3/4\pi^2)F_D(x=0)/NC_0U_0, \quad (1)$$

relates the sputtering yield  $Y$  to  $F_D$ , the deposited energy function (evaluated at  $x=0$ , i.e., at the target surface). A detailed discussion of  $F_D$  can be found in Ref. 8. For present purposes, it is sufficient to recall that  $F_D(x)dx$  represents the average kinetic energy left in *atomic motion*, in  $dx$  at  $x$  within the target, by a single ion.

At the time Eq. (1) was derived,  $F_D$  was calculated on the basis of the Lindhard-Scharff-Schiott (LSS) theory of collision cascades<sup>2</sup> using Lindhard's model of electronic energy losses where the electronic stopping cross section  $S_e$  is given by  $S_e = K_L v$  (where  $dE/dx = -NS_e$ ), and the Thomas-Fermi model for the projectile-atom and atom-atom interaction potentials.<sup>8</sup> With this electronic-loss-interatomic-potential model  $S_n$ , the nuclear stopping cross section is substantially greater than  $S_e$  at low energies; so the calculated  $F_D$  values did not show a strong dependence on the inelastic-loss cross section. This model introduces a low-energy region where electronic stopping can be neglected completely.

Later, when measurements of range profiles of low-energy ions became available,<sup>9</sup> disagreements between experiments and the calculations based on Thomas-Fermi potential showed that more strongly screened potentials, such as the Lenz-Jensen or Moliere functions, give better agreement between theory and experiment. Modern calculations and computer simulations use these potentials. The nuclear stopping power derived from these more strongly screened potentials decreases more rapidly at low

energy than those derived from Thomas-Fermi calculations; so with these potentials  $S_e$  would be comparable to, or even greater than,  $S_n$  at very low energies. This change should produce  $F_D$  values with a stronger dependence on  $S_e$  at low energy, but the calculations have not been repeated.

A recent computer simulation study<sup>10</sup> showed that the sputtering yield coefficient  $Y((\text{atoms})/(\text{ion}))$ , is very sensitive to electronic stopping energy losses calculated with  $S_e = K_L v$ , the same analytic form as the Lindhard model. Other computed "observables" are unaffected within the computational accuracy. Furthermore, it was demonstrated that  $Y$  is more sensitive to electronic energy losses by the *target atoms* than to such losses by the bombarding ions. The effect was demonstrated in two conceptually different simulation programs.

An alternative model of electronic energy losses, based on a modified version of the Firsov electronic energy-loss model,<sup>11</sup> which also leads to  $S_e = K_L v$ , was adopted in the MARLOWE (Ref. 3) series of computer simulations. It is usually called the "local-energy-loss model" (see below). It provides another calculational approach to the theoretical study of low-energy electronic losses. This local energy-loss model produces an electronic stopping power which decreases more rapidly with energy than Lindhard's or Firsov's at low energy; so the low-energy limit of  $S_e/S_n$  assumed in LSS theory is retrieved.

At present there is no direct experimental evidence supporting any of the Lindhard, Firsov, or modified Firsov energy-loss models *at low energy*.

The theoretical situation can be summarized as follows: the consensus seems to be that at low energy  $S_e$  should decrease more rapidly than  $S_n$ , but there is no experimental evidence supporting this conclusion, nor can any decision be made between the Lindhard (distributed loss) and Firsov (localized loss) models.

This paper examines the consequences of using  $S_e = K_L v$ , often with the Lindhard inelastic-loss approximation as an example, together with a strongly screened Coulomb potential. The next section discusses the modified *total deposited energy analysis*, the succeeding section deals with the *surface deposited energy*, and a final section compares the theoretical results with computations from computer simulations.

## II. THE INFLUENCE OF $S_e/S_n$ ON THE DEPOSITED ENERGY FUNCTION

### A. Background

The first step in a theoretical analysis of the influence of inelastic losses on atom ejection should necessarily start with the calculation of  $\nu(E)$ , because  $F_D$ , which is a major factor in the sputtering yield calculation, must satisfy

$$\int F_D(x)dx = \nu(E), \quad (2)$$

where  $\nu(E)$  is the total energy deposited in elastic collisions.

In the special case where the ion and target are the same element, and in the approximation where the bulk binding or displacement energy is neglected,  $\nu(E)$  obeys the following transport equation:

$$NS_e(E) \frac{d\nu}{dE} = N \int d\sigma_n [\nu(E-T) - \nu(E) + \nu(T)], \quad (3)$$

where  $N$  is the atomic number density in the target,  $T$  the energy transferred by a moving particle to a target atom, and  $d\sigma_n$  is the differential elastic scattering cross section.

Some results from two earlier calculations are summarized here to provide a basis for comparison with the new results. They also indicate the general philosophy of the new calculations.

To obtain a solution of Eq. (3), Lindhard, Nielsen, Scharff, and Thomsen<sup>12</sup> used the power approximation for the differential elastic scattering cross section:

$$N d\sigma_n = NC_m dT / (E^m T^{m+1}), \quad (4)$$

and an electronic stopping cross section proportional to the velocity:

$$S_e(E) = Kv, \quad (5)$$

where

$$v = (2E/M_1)^{1/2} \\ K = K_L = 8\pi e^2 a_0 Z_1 Z_2^{7/6} / Zv_0. \quad (6)$$

Here  $M_1, M_2$  are the ion and atom masses, respectively,  $Z_1, Z_2$  are the corresponding atomic numbers,  $a_0$  is the Bohr radius,  $v_0$  the Bohr velocity, and

$$Z = (Z_1^{2/3} + Z_2^{2/3})^{3/2}.$$

In this derivation,  $K$  need not be  $K_L$ , but we do require that  $S_e$  be proportional to the velocity.

From Eq. (5) they determined that

$$\nu(E) = EF(2/(4m-1), (2m+1)/(4m-1), \\ (2m+3)/(4m-1), -\xi(E)), \quad (7)$$

where

$$\xi(E) = S_e(E)/S_n(E) \propto E^{2m-1/2}, \quad (8)$$

and  $F(a, b, c, d)$  is the hypergeometric function. The same authors calculated  $\nu(E)$  exactly by solving Eq. (3) numerically, using a more general elastic collision cross section. Sigmund, Matthies, and Phillips<sup>13</sup> proposed a series ex-

pansion for  $\nu(E)$ , valid at low energies:

$$\nu(E) = E(1 + c_1 K + c_2 K^2 + \dots). \quad (9)$$

They calculated the coefficients in Eq. (9), then solved Eq. (3) numerically, using Eq. (9) as the boundary condition. They found that a two-term series produced sufficient accuracy in the numerical integration. From the completed analysis, they obtained

$$\nu(E) \simeq E \left[ 1 - \frac{2KE^{2m-1/2}}{K_1(m, 2m + \frac{3}{2})NC_m} \right], \quad (10)$$

where

$$K_1(m, 2m + \frac{3}{2}) = (2m + \frac{1}{2})/[m(m + \frac{1}{2})] \\ - B(2m + \frac{3}{2}, -m),$$

and  $B(a, b)$  is the beta function.

Both of these calculations depend upon the following assumption:

$$S_e/S_n \rightarrow 0 \text{ as } E \rightarrow 0. \quad (11)$$

When this condition is fulfilled,  $\nu(E) = E$  as  $E \rightarrow 0$ . In this model there exists a low-energy range, where electronic stopping can be neglected.

At low energy, we know that a power potential with  $m \geq \frac{1}{3}$  overestimates the elastic interaction, and that powers of  $m < \frac{1}{3}$  must be used. This has been clearly demonstrated in the analysis of low-energy heavy-ion range measurements,<sup>9,14</sup> and there are also theoretical reasons which support such a limitation. This limitation is important here, because as soon as  $m \leq \frac{1}{4}$  the condition contained in Eq. (11) is no longer satisfied, see Eq. (8). Therefore, *no expansion in powers of  $S_e/S_n$* , which is basic to both of these calculations, *can be a good approximation at low energy*. This behavior is reflected in Eqs. (7) and (10), where both formulae break down for  $m \leq \frac{1}{4}$ .

Fortunately, this limitation is not a problem in practical computations and most computer simulations, because in both cases motion is followed only so long as a particle has an energy greater than  $E_0$ , where  $E_0$  is an arbitrary threshold, or cut-off, energy.

The singularity also would be easily eliminated if  $S_e$  were allowed to decrease faster than  $S_n$ . However, the extent to which one can modify the velocity-proportional stopping power at low energy remains poorly understood.

### B. Calculations

Here we calculate  $\nu(E)$  using power potentials with  $m \leq \frac{1}{4}$ . This will allow us to examine the withdrawal of kinetic energy from the atoms of a low-energy cascade by inelastic (electronic) processes.

To avoid the complications introduced by the fact that Eq. (11) is not satisfied for small-power potentials, we introduce a threshold energy,  $E_0$ . Unfortunately, there is no unique way to define  $E_0$ . We know from radiation-induced damage studies in solids that there are several candidate threshold energies. For example, the solid binding energy (cohesive energy) and the displacement energy immediately come to mind. Another possibility is the

direct cutoff of kinetic energy, as used in most of the Monte Carlo computer simulations.

For the sake of simplicity, here we will adopt the criteria that the electronic stopping power will be turned off as soon as the kinetic energy of a particle falls below  $E_0$ . Formally:

$$S_e(E) = \begin{cases} 0, & E < E_0 \\ K(2E/M_1)^{1/2}, & E \geq E_0 \end{cases} \quad (12)$$

Using this relation, we write Eq. (3) as:

$$\Theta(E - E_0)K \left( \frac{2E}{M_1} \right)^{1/2} \frac{d\nu(E)}{dE} = \int d\sigma_n [\nu(E - T) - \nu(E) + \nu(T)], \quad (13)$$

where  $\Theta(x)$  is the Heaviside unit step function. Equation (13) ensures that, for  $E < E_0$ ,  $\nu(E) = E$  whether or not Eq. (11) is satisfied. To find an analytic solution to Eq. (13), we closely follow Signmund's procedure.<sup>13</sup> We also introduce a power-series expansion:

$$\nu(E) = \sum_i C_i(E)K^i, \quad (14)$$

where  $K$  is the electronic stopping coefficient; see Eq. (5). When Eq. (14) is introduced into Eq. (13), we equate the terms of equal powers of  $K$  on both sides of the equation, and obtain the set of equations:

$$\Theta(E - E_0) \left( \frac{2E}{M_1} \right)^{1/2} \frac{dC_{i-1}}{dE} = \int d\sigma_n [C_i(E - T) - C_i(E) + C_i(T)]. \quad (15)$$

The first coefficient,  $C_0$ , represents the limit of no electronic energy loss; therefore,  $C_0 = E$ . To calculate  $C_1$ , replace  $d\sigma_n$  by the power approximation, Eq. (4). Then Eq. (15) reads:

$$\Theta(E - E_0) \left( \frac{2E}{M_1} \right)^{1/2} = \frac{C_m}{E^m} \int \frac{dT}{T^{m+1}} [C_1(E - T) - C_1(E) + C_1(T)]. \quad (16)$$

Equation (16) can now be solved using the Laplace transformation technique,<sup>15</sup> which allows us to find the leading terms in a series expansion in powers of  $(E/E_0)$ . Omitting the details, the results are as follows.

(1) For the  $4m - 1 > 0$  case:

$$\nu(E) \simeq E \left\{ 1 - \frac{12}{(4m-1)\pi^2} \left[ \left( \frac{S_e(E)}{S_n(E)} \right) \frac{2}{(4m+1)} - \frac{S_e(E_0)}{S_n(E_0)} \right] \right\}. \quad (17)$$

(2) For the  $4m - 1 = 0$  case:

$$\nu(E) \simeq E \left\{ 1 - \frac{6}{\pi^2} \left( \frac{S_e(E)}{S_n(E)} \right) \left[ \ln \left( \frac{E}{E_0} \right) - 1 \right] \right\}. \quad (18)$$

(3) For the  $4m - 1 < 0$  case:

$$\nu(E) \simeq E \left[ 1 - \frac{12}{(1-4m)\pi^2} \left( \frac{S_e(E_0)}{S_n(E_0)} - \frac{2S_e(E)}{(4m+1)S_n(E)} \right) \right]. \quad (19)$$

If we take Eq. (8) into account, and assume that  $2m - 1/2 \ll 1$ , the three solutions reduce (approximately) to a single expression:

$$\nu(E) \simeq E \left[ 1 - \frac{6}{\pi^2} \frac{S_e(E)}{S_n(E)} \ln \left( \frac{E}{E_0} \right) \right], \quad (20)$$

where the  $m$  dependence is all contained in  $(S_e/S_n)$ . Close examination of Eq. (17) indicates that it yields practically the same results as Eqs. (10) and (7) when  $E_0$  tends to zero. The difference, a consequence of the Laplace transformation technique employed to obtain Eq. (17), remains less than 10% for all three cases. Note that the chief difference between this analysis and those previously published is the introduction of the energy scaling threshold,  $E_0$ .

### C. Results

The preceding analysis removes the anomaly contained in the earlier calculations which limited the study of the energy deposited in elastic collisions to power potentials where  $m \geq \frac{1}{4}$ . To interpret the results given in Eqs. (17)–(19) and summarized in Eq. (20), we restate the equations in terms of Lindhard's well-known reduced energy  $\epsilon$ , so that all target and projectile dependencies are contained in the transformation law:

$$\epsilon = \frac{aE}{(1 + M_1/M_2)Z_1Z_2e^2}, \quad (21)$$

where

$$a = 0.8853a_0 / (Z_1^{2/3} + Z_2^{2/3})^{1/2},$$

$a_0 = 5.29$  nm, is the Bohr radius,  $M_1$  and  $M_2$  are the projectile and target masses respectively, and  $Z_1$  and  $Z_2$  are their atomic numbers. As before, set  $M_1 = M_2$  and  $Z_1 = Z_2$ .

The electronic and nuclear stopping can now be written as

$$s_e(\epsilon) = k\epsilon^{1/2}, \quad (22a)$$

$$s_n(\epsilon) = \frac{\lambda_m \epsilon^{1-2m}}{2(1-m)}, \quad (22b)$$

where the  $(m, \lambda_m)$  values are chosen in such a way that Eq. (22b) approximates the nuclear stopping power within different intervals of  $\epsilon$ . In particular, the  $(m, \lambda_m)$  chosen are those of Ref. 16, so that Eq. (22b) will approximate the low-energy limits of the Thomas-Fermi, Moliere, or

Lenz-Jensen nuclear stopping powers as required.

Except for light particles, the electronic-loss coefficient,  $k$ , is a smooth function of the projectile and target species; so setting  $k = 0.15$  will serve as a representative value.

At this point the threshold energy  $E_0$  and the corresponding reduced threshold  $\epsilon_0$  have still not been determined; so we consider values of  $\epsilon_0$  where  $10^{-5} < \epsilon_0 < 10^{-6}$ , which covers a range of threshold energies from a few eV to a few tens of eV.

Eq. (16) has been evaluated both numerically and analytically. The results are plotted in Figs. 1 and 2 in the form of  $\nu(\epsilon)/\epsilon$ , which is the fraction of the energy deposited into elastic collisions. The "elastic limit," where  $\nu(\epsilon)/\epsilon = 1$ , is also indicated. It represents the case of  $k = 0$ , where there is no inelastic loss.

For the three screened Coulomb potentials being considered here, the screening increases in the order: Thomas-Fermi, Moliere, and Lenz-Jensen. From the variation of  $\nu(\epsilon)/\epsilon$  with  $\epsilon$  in Figs. 1 and 2 it is clear that a strong correlation exists between stronger screening and the magnitude of inelastic losses, because  $\nu(\epsilon)/\epsilon$  would be exactly one if inelastic (electronic) effects were not present. Not surprisingly, the potentials most sensitive to the  $\epsilon_0$  value are those with stronger screening, that is, the Moliere and Lenz-Jensen. For the Thomas-Fermi potential,  $\nu(\epsilon)$  practically does not depend on  $\epsilon_0$  at all. Furthermore, qualitatively, the curves are dependent only slightly on the choice of  $\epsilon_0$ ; so the threshold energy is not a sensitive parameter of the analysis.

The dependence of the shape on  $\epsilon_0$  indicates that, for the Moliere and Lenz-Jensen potentials, most of the energy loss to electronic excitation occurs at low-particle energy. In a cascade the major fraction of the energy losses to electronic processes is produced by low-energy recoil atoms rather than by the incoming ion or the energetic PKA's. This conclusion is emphasized because it contradicts the assumed low- $m$  behavior inferred from the  $m > \frac{1}{4}$  analysis by most workers in the field. Although the electronic stopping power is smaller at low energies (but still

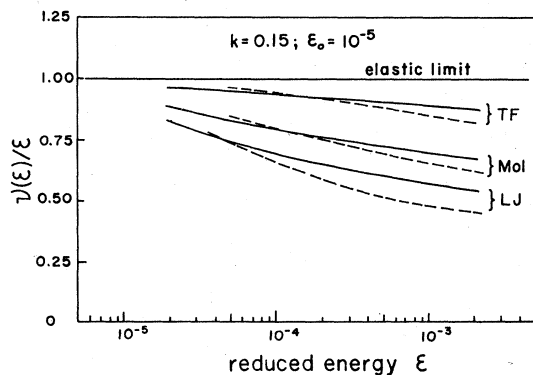


FIG. 1. Fraction of the energy deposited into elastic collisions,  $\nu(\epsilon)/\epsilon$ , as a function of the reduced energy  $\epsilon$ . Lindhard electronic coefficient  $k = 0.15$  and inelastic energy loss threshold  $\epsilon_0 = 10^{-5}$ . Solid line: exact numerical calculation. Dashed line: approximate solution [Eq. (20)]. Both ion and target are assumed to be the same element.

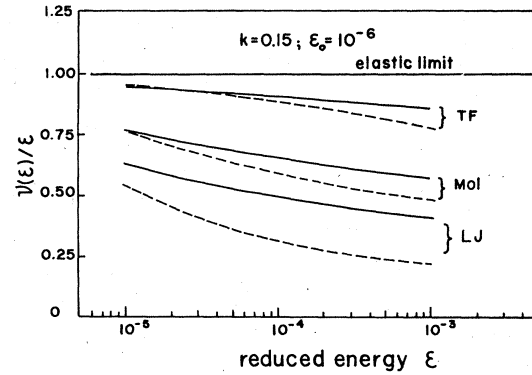


FIG. 2. Same as Fig. 1,  $\epsilon_0 = 10^{-6}$ .

with  $\epsilon \geq \epsilon_0$ ), the number of low-energy particles in the system is very much greater than the number of high-energy ones; so the effect of the many small contributions is greatly magnified.

There is a double sensitivity here, to  $m$  and to  $\epsilon_0$ . Consider the  $\epsilon_0$  sensitivity first. A decrease in  $\epsilon_0$  implies that an inelastic loss persists through more collision generations; so the number of moving atoms is decreased. This is an important clue, which helps to explain the  $m$  dependence. It also is important to remember that inelastic stopping is a *one-way* flux of energy. Each time a recoil atom loses an amount of energy to electronic processes, that energy is effectively removed from the dynamical system;<sup>17</sup> so it is unavailable to affect later elastic collisions. Nuclear collisions do not behave this way; energy remains available for further dynamical events. *Only when the energy transferred during a collision is less than  $\epsilon_0$  can one be sure that none of it will end up as electronic excitations.*

A simple, approximate, analytic calculation of  $\nu(E)$  which avoids the use of integral equations illustrates this argument. Suppose that a recoil has been produced with kinetic energy  $E'$ . The total amount of energy which this recoil atom subsequently loses to electronic processes (before its energy falls below the threshold,  $E_0$ ) is given by:<sup>18</sup>

$$\eta_1(E') \cong \int_{E_0}^{E'} dE'' \frac{NS_e(E'')}{[NS_e(E'') + NS_n(E'')]} \quad (23)$$

If  $S_n \gg S_e$  this reduces to

$$\eta_1(E') \cong \int_{E_0}^{E'} dE'' \frac{S_e(E'')}{S_n(E'')} \quad (24)$$

Now by using the results of Eqs. (22a) and (22b), Eq. (24) becomes

$$\eta_1(E') \cong \frac{E'S_e(E')}{(2m + \frac{1}{2})S_n(E')} \quad (25)$$

On the other hand, an ion of energy  $E$  is known to produce a cascade with an energy spectrum approximately given by<sup>19</sup>

$$\frac{dn}{dE'} \cong \frac{6}{\pi^2} \frac{\nu(E)}{(E')^2}, \quad (26)$$

where, for the purpose of this analysis, we can set

$\nu(E)=E$ . Then the total energy deposited into electronic excitations by *all recoil atoms* can be obtained from the expression:

$$\begin{aligned} \eta(E) &\simeq \frac{6}{\pi^2} \int_{E_0}^E dE' \frac{\eta_1(E')}{E'^2} \\ &\simeq \frac{6E}{\pi^2} \frac{S_e(E)}{S_n(E)} \frac{\ln(E/E_0)}{(2m + \frac{1}{2})}. \end{aligned} \quad (27)$$

Finally,

$$\nu(E) = E - \eta(E) \simeq E \left[ 1 - \frac{6}{\pi^2} \frac{S_e(E) \ln(E/E_0)}{(2m + \frac{1}{2}) S_n(E)} \right]. \quad (28)$$

#### D. Discussion and Conclusions

Mathematically, Eq. (28) approximates Eq. (20) very well. In Eq. (28) it is interesting to observe that the energy deposited into electronic excitations by the low-energy portion of the cascade dominates through the factor  $(E')^{-2}$  in the integral of Eq. (27). From either approach, one concludes that to ignore electronic stopping in the determinations of  $\nu(E)$  can introduce major errors, especially when the "realistic" screened Coulomb potentials are used.

Another important consequence of this analysis follows from the previously mentioned fact that a small power,  $m$ , produces a correspondingly smaller nuclear stopping, thereby increasing the dependence of  $\nu(E)$  on electronic stopping. In this respect, the often-used assumptions that the low-energy cascade develops in the elastic limit, and the power law  $m=0$  is appropriate for low-energy particles,<sup>20</sup> are both questionable. The unavoidable conclusion is that the existence of an elastic limit is no longer demonstrable.

Since low  $\epsilon_0$  values are generally obtained within cascades on high- $Z$  targets, it follows from these results that electronic processes would be more effective in high- $Z$  materials, rather than in low- $Z$  materials. This result also is at variance from the usual assumption in which inelastic stopping is only considered for light particles.

Finally, we note that although the approximate solutions, Eq. (20), follow the exact numerical calculations fairly well, there are some deviations in the case of the Lenz-Jensen potential. The difference can be attributed to the large value of  $S_e/S_n$ , for which the series expansion, Eq. (14), converges poorly. In all cases, one should expect that Eq. (20) will underestimate  $\nu(E)$  at large energies, because it only contains terms up to the first order in the electronic stopping power. The next, quadratic term in  $S_e/S_n$ , should be positive.

This approach to inelastic energy losses can be summarized as follows. By introducing a threshold energy  $E_0$  below which there will be no electronic stopping, the total energy deposited in elastic collisions by particles obeying strongly screened Coulomb interactions can be calculated. These results show that in the cases of the Moliere and Lenz-Jensen potentials, the energy lost to electronic excitations by low-energy particles in the cascade amounts to about 50% of the total available energy.

The analysis also indicates, see Eq. (28), that the magnitude of  $S_e$  is a less significant variable than the ratio  $S_e/S_n$  in the determination of  $\nu(E)$ . A great deal more attention needs to be paid to the ratio in future calculations of this sort. Although the calculations are based on the Lindhard-stopping power law, owing to the large number of the low-energy recoil atoms, the electronic stopping of low-energy particles will have a great influence on the fraction of energy elastically deposited for any electronic stopping model.

### III. THE SURFACE DEPOSITED ENERGY $F_D$ AS A FUNCTION OF $S_e/S_n$

#### A. Background

The preceding section deals with the  $S_e/S_n$  dependence of the energy distribution in a collision cascade, and demonstrates that there can be a strong dependence at low energies. This section is more specialized. It concentrates on the *surface-deposited energy*  $F_D$  as defined by Winterbon,<sup>8</sup> which is a major factor in the sputtering process. It demonstrates that  $F_D$  exhibits the dependence discussed above. This similarity is to be expected, but further insight into low-energy inelastic processes can be gained by working out some of the details of the  $F_D$  analysis.

There are basically two reasons why the surface-deposited energy depends on  $S_e/S_n$ : first, the *form* of the deposited energy distribution has been shown to be dependent on  $S_e/S_n$ ; and second, as demonstrated above, the *magnitude* of the deposited energy function, which is proportional to the total number of moving atoms, depends on the ratio, so the energy deposited by *nuclear* collisions will be less than for the purely elastic model, because the ion's energy ultimately is partitioned between atomic displacements and electronic excitations.

#### B. Calculations

As mentioned above,  $F_D$  has been calculated previously only for interatomic potentials such that at low energies the corresponding  $S_n$  remains substantially greater than  $S_e$ . As soon as a more strongly screened Coulomb potential is employed, Lindhard's form of  $S_e$  becomes comparable to  $S_n$ , and noticeable effects on  $F_D$  can be anticipated.

The complete  $F_D$  calculation represents a complicated numerical procedure which involves the solution of a system of integro-differential equations for the spatial moments of the Legendre function expansion of  $F_D$  on the directional cosine of the incoming ion's velocity. Some simple estimates show that the complete analysis is not required to examine the  $S_e/S_n$  dependence.

The approximation can be developed as follows: Because  $F_D$  must be normalized to the energy deposited in all elastic collisions,  $\nu(E)$ , we wrote Eq. (2) in the form:

$$\nu(E) = \int_{-\infty}^{+\infty} F_D(x) dx,$$

so a legitimate approximation for  $F_D$  can be written as

$$F_D(x=0) \simeq \frac{\nu(E)}{\langle (\Delta x)^2 \rangle^{1/2}}, \quad (29)$$

where  $\langle(\Delta x)^2\rangle^{1/2}$  describes the spatial extension of the deposited energy distribution along the  $x$  axis. In this expression electronic stopping can change  $F_D(x=0)$  in either of the two ways, directly through  $\nu(E)$  or indirectly through  $\langle(\Delta x)^2\rangle^{1/2}$ . Now we investigate these two dependencies in greater detail.

The distribution width  $\langle(\Delta x)^2\rangle^{1/2}$  is chiefly determined by the most energetic particles in the cascade, in this case, the bombarding ion. Now we obviate the need to perform the difficult direct computation of  $\langle(\Delta x)^2\rangle^{1/2}$  by taking advantage of its known similarities to the range  $\langle R \rangle$  and the range straggling  $\langle(\Delta R)^2\rangle$ .

From the preceding analysis, we anticipate that both  $\langle R \rangle$  and  $\langle(\Delta R)^2\rangle$  will be sensitive to inelastic effects through  $S_e(E)/S_n(E)$ . If this is the case, one expects that  $\langle(\Delta x)^2\rangle^{1/2}$  will behave similarly. We shall now examine the behavior of  $\langle R \rangle$  and  $\langle(\Delta R)^2\rangle$  in the presence of inelastic effects.

These functions can be calculated from the equations:

$$\langle R \rangle \cong \int_{E_0}^E dE' / N(S_e + S_n), \quad (30)$$

and

$$\langle(\Delta R)^2\rangle = \int_{E_0}^E dE' N \Omega_n^2 / (NS_e + NS_n)^3, \quad (31)$$

where  $N$  is again the atomic density in the solid, and

$$\Omega_n^2 = \int T^2 d\sigma_n \quad (32)$$

is the nuclear straggling cross section. The standard derivation also assumes that the electronic *straggling* cross section  $\Omega_e^2$  is smaller than  $\Omega_n^2$ ; so that its effect on  $\langle(\Delta R)^2\rangle$  can be neglected.

To calculate Eqs. (30) and (31), it is convenient to introduce reduced units, see Eq. (21) above. Accordingly Eq. (30) becomes

$$\langle \rho \rangle = \int_{\epsilon_0}^{\epsilon} d\epsilon' / [s_e(\epsilon') + s_n(\epsilon')], \quad (33)$$

and Eq. (31) becomes

$$\langle(\Delta \rho)^2\rangle = \gamma \int_{\epsilon_0}^{\epsilon} d\epsilon' \omega_n^2(\epsilon') / [s_n(\epsilon') + s_e(\epsilon')]^3, \quad (34)$$

where  $\gamma = 4M_1M_2 / (M_1 + M_2)^2$ . Furthermore,

$$s_n = (1/\epsilon) \int_0^{\epsilon} f(x) dx, \quad (35)$$

$$s_e = k\epsilon^{1/2}, \quad (36)$$

and

$$\omega_n^2(\epsilon) = (1/\epsilon^2) \int_0^{\epsilon} x^2 f(x) dx. \quad (37)$$

Next replace  $f(x)$  by the power approximation,  $f(x) = \lambda_m x^{1-2m}$  and evaluate Eqs. (32) and (33). Figure 3 shows the resultant functions in the form  $\langle \rho(k=0.2) \rangle / \langle \rho(k=0) \rangle$  and  $[\langle(\Delta \rho^2)(k=0.2) \rangle / \langle(\Delta \rho^2)(k=0) \rangle]^{1/2}$  to emphasize the inelastic loss dependence. As above, the calculations were performed with three different values of  $m$ , corresponding to the low-energy limit of the Thomas-Fermi, Moliere, and Lenz-Jensen potentials, respectively. As the results appear to be insensitive to the  $\epsilon_0$  value, set  $\epsilon_0 = 0$ . Note that  $k=0.2$  represents a "worst case," where the electronic energy loss

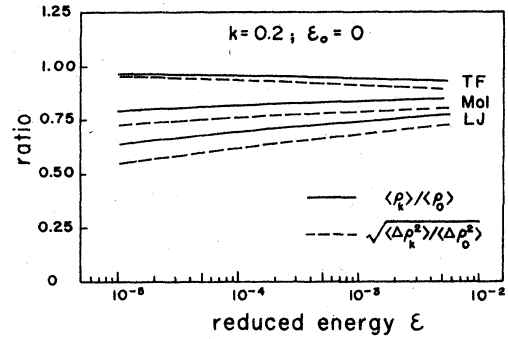


FIG. 3. This figure illustrates the relative change of the range,  $\langle \rho \rangle$ , and range straggling,  $\langle(\Delta \rho)^2\rangle$ , as functions of the reduced energy  $\epsilon$  due to Lindhard's inelastic losses with  $k=0.2$  [see Eq. (22a)].

is very strong.

Comparing the effect of inelastic energy losses on  $\nu(E)$ ,  $\langle \rho \rangle$ , and  $\langle(\Delta \rho)^2\rangle$ , see Figs. 1–3, it is evident that  $\nu(E)$  is the most sensitive. This means that electronic effects cannot be expected to cancel out of Eq. (29), because the numerator and denominator depend on them in different ways.

#### D. Discussion

When these results are considered in conjunction with Eq. (1), it is reasonable to presume that, as for  $S_e(E)$ , the sputtering yield coefficient,  $Y$ , should be proportional to the total energy deposited elastically. Any effect observed on  $\nu(E)$ , as a consequence of changing either the projectile or target electronic stopping power, should also be observed in the calculated yield. Conversely, many of the implications that inelastic effects have for sputtering can be anticipated from the corresponding effects on  $\nu(E)$ .

#### IV. APPLICATIONS TO SPUTTERING

We are now in a position to analyze the inelastic low-energy effects in our sputtering yield simulations<sup>10</sup> in terms of the modifications which energy losses to electronic processes have introduced into  $\nu(E)$  and  $F_D$ . These computations showed that the sputtering yield  $Y$  is more sensitive to inelastic losses by the atoms of the target than to losses by the incident ion.

Two logically different simulations, QDYN (Ref. 21) and TRIM.SP (Ref. 22), were run on Cu(111) and amorphous Cu targets, respectively, with different 3.0-keV ions. Results were computed for a set of trajectories with electronic losses "on" for both ions and atoms. The same trajectories were then first repeated with ion losses on and atom losses "off", then with ion losses off and atom losses on, and finally with both atom and ion losses off. The computations result in four sputtering yield coefficients:  $Y(1,1)$ ,  $Y(1,0)$ ,  $Y(0,1)$ , and  $Y(0,0)$ . In this notation, "0" indicates that the electronic processes were off,  $K=0$ , and "1" means that  $K=K_L$ , where  $K_L$  is the Lindhard electronic stopping coefficient; see Eq. (5). These results, for a number of ions, have been plotted in Fig. 4 as *relative sputtering yields*,  $Y(i,j)/Y(0,0)$ , where the "no-loss"

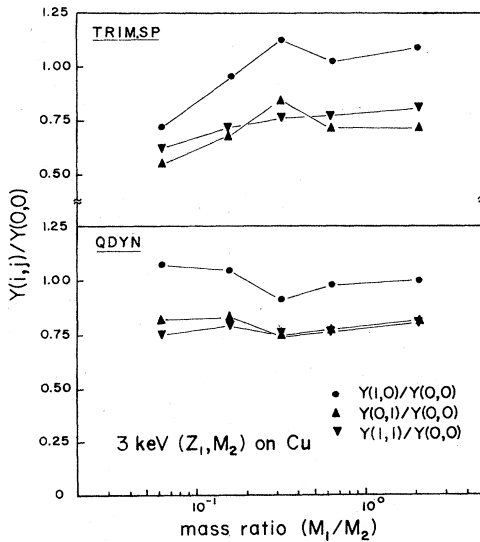


FIG. 4. Sputtering yield ratios for different 3.0-keV ions on a Cu target obtained from (a) QDYN and (b) TRIM.SP simulations.  $Y(1,0)$ : yield calculated including inelastic losses of the ion alone.  $Y(0,1)$ : atoms alone.  $Y(1,1)$ : both ion and atoms.  $Y(0,0)$ : no inelastic losses.

case is used as a standard.

Figures 4 and 5 show the same type of results for 3.0-keV Ar bombarding different targets. Each target atom-atom potential function consists of a "0.8 Moliere" wall joined smoothly to a Morse potential attractive well,<sup>21</sup> so binding and displacement energies are included in the simulations.

The calculations have allowed us to investigate the importance of electronic stopping of low-energy recoils, but direct comparisons between the computed yield values and theory are not possible, because Eqs. (16)–(19) were for

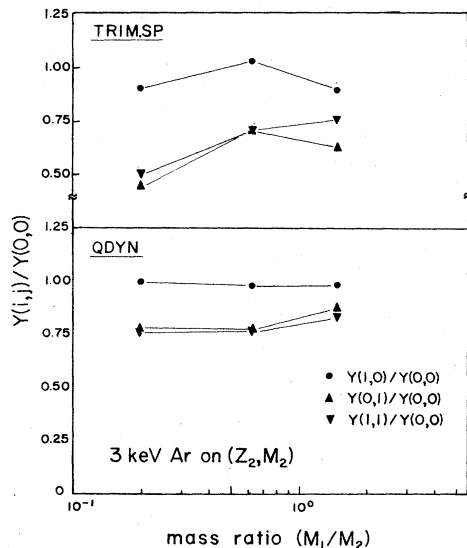


FIG. 5. Same as Fig. 4 for 3.0-keV Ar on different targets.

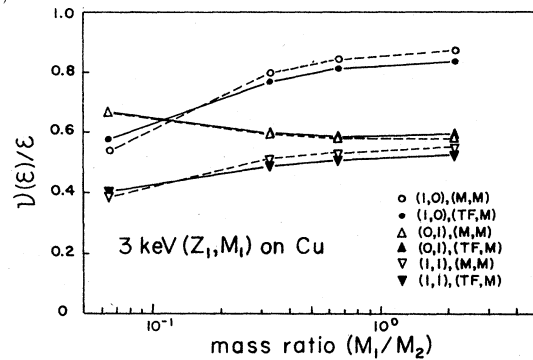


FIG. 6. Fraction of the energy deposited into elastic collisions for different 3.0-keV projectile on a Cu target. Solid line: exact numerical calculations. Dashed line: approximate solution [Eq. (20)]. The 0's and 1's in the first parenthesis stand for the inelastic losses of the ion and atoms, respectively; see caption of Fig. 4. The letters in the second parenthesis indicate the potential employed for the ion-atom and atom-atom interaction, respectively. M, Moliere; TF, Thomas-Fermi.

the case when the ions and atoms were the same species. To make a more direct comparison, we must calculate the total energy elastically deposited by an arbitrary ion,  $v_1(E)$ . This can be done directly from the expression

$$v_1(E) = \int_{E_0}^E \frac{dE'}{NS_n^{(1)} + NS_e^{(1)}} \left| \frac{dv_1}{dR} \right|, \quad (38)$$

where  $NS_n^{(1)}$  and  $NS_e^{(1)}$  are the nuclear and electronic stopping cross sections of the ion, and

$$\left| \frac{dv_1}{dR} \right| = N \int d\sigma_n^{(1)}(E, T) v(T). \quad (39)$$

Here  $v(T)$  is the energy elastically deposited by a recoil ion with initial energy  $T$ , and  $d\sigma_n^{(1)}(E, T)$  is the differential elastic scattering cross section of the ion as a function of the ion energy  $E$  and the energy transferred  $T$ .

Figures 6 and 7 show the results of evaluating Eq. (38) numerically for 3.0-keV Ar on different targets and for different 3.0-keV ions on a Cu target. The same notation used in Figs. 4 and 5 is used to label the curves: (0,1) represents the case where there is no inelastic loss for the ion, and the recoil atom's electronic stopping is given by

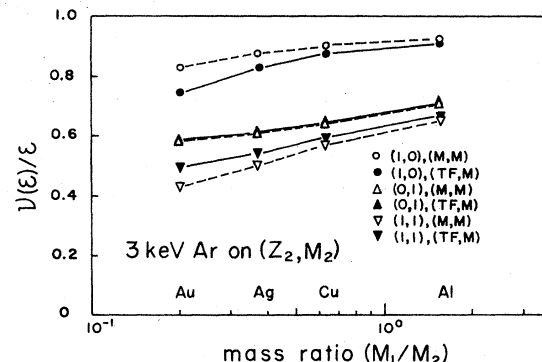


FIG. 7. Same as Fig. 6 for 3.0-keV Ar on different targets.



Lindhard's approximation, etc. Since there are now two kinds of interactions, a second parenthesis indicates which interatomic potential has been used.

The similar behavior of  $\nu_1(E)$  and  $Y$  (see Figs. 4–7) corroborates the proportionality that exists between the two quantities. As discussed in Ref. 10, the results shown in Figs. 4–7 demonstrate that the electronic stopping of low-energy recoil atoms has greater influence on the sputtering yield than the electronic stopping of the ion.

Figure 8 shows the sensitivity of the sputtering yield to  $E_0$ , the stopping threshold. The calculations were done using the TRIM.SP simulation code, with different values of  $E_0$ . In the program, the stopping coefficient was defined as

$$NS_e = \begin{cases} NS_e(\text{Lindhard}), & E > E_0 \\ 0, & \text{otherwise.} \end{cases} \quad (40)$$

Here  $E$  is the instantaneous energy of the Cu atom in the cascade.

Note the logarithmic scale in Fig. 8. We see that  $Y$  diminishes slowly above 20 eV, and then more rapidly when  $Y$  is roughly halfway between the no-loss and full-loss limiting values. The striking result is that the sputtering yield for  $E_0 = 500$  eV is almost the same as that corresponding to the no-loss case. This is direct confirmation of the importance of the losses by the low-energy recoil atoms. In the particular case depicted in Fig. 8, 80% of the electronic stopping contributions occurs for recoils having energies less than roughly 200 eV. Thus electronic effects are important for low-energy particles as well as for light ions.

Formally, all of these calculations were carried out with the Lindhard electronic stopping power, but the conclusions do not depend on that choice<sup>10</sup> so long as  $S_e \propto v$ . This independence is important, because some authors<sup>7,23,24</sup> have questioned the applicability of Eq. (5), the Lindhard electronic stopping power formula, to low-energy atomic motion, and have used Firsov's model of electronic losses<sup>10</sup> to show that the Lindhard formula could overestimate the electronic stopping at low-particle velocities. Both the Firsov and Lindhard models predict a loss exactly proportional to  $v$ .

Robinson and Torrens<sup>3</sup> and Oen and Robinson,<sup>25</sup> in the local inelastic loss model, approximated Firsov's model by

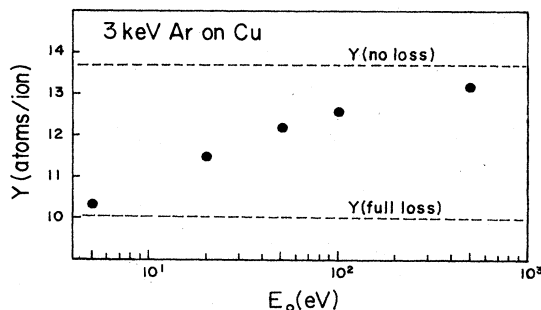


FIG. 8. Sputtering yield obtained with TRIM.SP simulation for 3.0-keV Ar on Cu, as a function of the inelastic energy loss threshold,  $E_0$ . See the text.

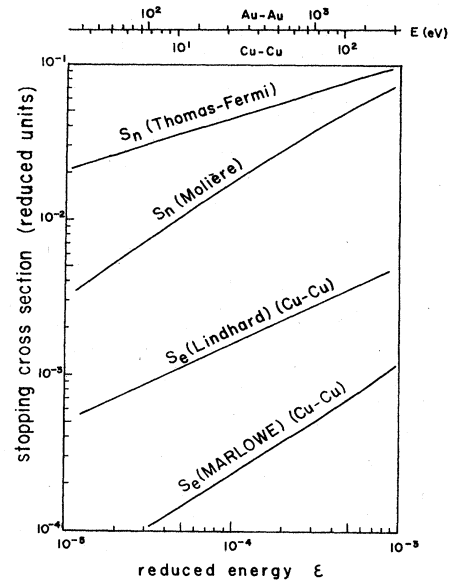


FIG. 9. Reduced electronic and nuclear stopping power as a function of the reduced energy  $\epsilon$ .

replacing the impact parameter with the distance of closest approach. In this version of electronic losses, the stopping power decreases more rapidly than  $E^{1/2}$ .

Figure 9 compares the Lindhard and MARLOWE electronic stopping power, and also nuclear stopping powers calculated from the Thomas-Fermi and Molière interaction potential, all as functions of the reduced energy. The nuclear stopping-power calculations were performed with the TRIM.SP program, using the MARLOWE energy loss. Sputtering yields calculated in this way are almost indistinguishable from the no-loss cases discussed above. This result is as anticipated from the  $\nu(E)$  studies, since  $S_e(\text{MARLOWE})/S_n$  goes rapidly to zero with decreasing energy, even for strongly screened potentials.

## V. SUMMARY AND CONCLUSIONS

This paper shows that the strong electronic loss dependence of sputtering demonstrated by two simulation programs is consistent with existing analytic theories of atomic collision cascades and sputtering, and could have been anticipated, had the low-energy sections of the theories been developed in slightly different form.

This dependence becomes detectable when the ratio of the electronic stopping power to the nuclear stopping power,  $S_e(U_0)/S_n(U_0) > 10^{-1}$ . Both cross sections are evaluated at the binding energy,  $U_0$ . When the ratio exceeds this value, the number of low-energy moving particles is significantly reduced, and detectable reductions are observed in the sputtering yield.

Our results are in total agreement with those contained in a recent similar investigation performed by Biersack and Eckstein.<sup>22</sup> Using a different version of the TRIM.SP, which includes inelastic energy losses in the selvage as well as in the bulk, they found that the sputtering yield was very sensitive to the energy-loss approximation employed in the simulations, and showed that inelastic ener-

gy losses of the sputtered atoms as they traverse the electron selvage at the surface decrease the sputtering yield by 25%. Neither QDYN, nor the version of TRIM.SP which we have been running, include provisions for inelastic energy losses in the electron selvage at the surface. The effects observed in our computations are consequences of electronic stopping effects *in the bulk*, during the collision cascade, which is not a surface effect.

We are led to conclude that existing cascade theory is not complete for situations in which the results depend sensitively on the properties of the low-energy particles in the cascade, as in sputtering theory. A theory designed to deal with processes which occur late in the cascade must include inelastic, nonconservative processes as well as the usual collision cascade dynamical analysis. Because existing sputtering theory developed in parallel with the theory of atomic cascades in solids, which is primarily concerned with the calculation of particle ranges, it tends to overemphasize the importance of the high-energy portion of the collision cascade.

This investigation is not meant to be a complete theoretical rederivation of analytic cascade theory. The

analysis has been limited to factors which directly impact the atom ejection processes. The desirability of a complete redevelopment of much existing theory has been indicated, but such an effort is beyond our more limited objectives. This paper addresses the single issue of the theoretical interpretation of the marked inelastic loss effects observed in the sputtering simulations.

*Note added in proof:* After the manuscript was accepted we found a paper by M. S. Miller and J. W. Boring [Phys. Rev. A 9, 2421 (1974)] which uses similar mathematical techniques to discuss the amount of energy that goes into electronic processes during the slowing down of keV ions in gases. Their findings are in total agreement with the calculations contained in Sec. II.

#### ACKNOWLEDGMENTS

This investigation was supported by a Special Research Opportunity Grant from the U.S. Office of Naval Research, Department of the Navy and by the Foundation Research Program of the Naval Postgraduate School (Monterey, Ca).

\*Permanent Address: Centro Atómico Bariloche, Comisión Nacional de Energía Atómica, 8400 Bariloche, Argentina.

<sup>1</sup>P. Sigmund, in *Sputtering by Particle Bombardment I*, edited by R. Berisch (Springer, Berlin, 1981).

<sup>2</sup>J. Lindhard, M. Scharff, and H. E. Schiøtt, K. Dan. Vidensk. Selsk. Mat. Fys. Medd. 33, 14 (1963).

<sup>3</sup>M. T. Robinson and I. M. Torrens, Phys. Rev. B 9, 5008 (1974).

<sup>4</sup>M. T. Robinson, J. Appl. Phys. 54, 2650 (1983).

<sup>5</sup>P. Sigmund, Phys. Scr. 28, 257 (1983).

<sup>6</sup>H. H. Anderson and H. L. Bay, in *Sputtering by Particle Bombardment I*, edited by R. Berisch (Springer, Berlin, 1981).

<sup>7</sup>M. T. Robinson, J. Appl. Phys. 54, 2650 (1983).

<sup>8</sup>K. B. Winterbon, P. Sigmund, and J. B. Sanders, K. Dan. Vidensk. Selsk. Mat. Fys. Medd. 37, 14 (1970).

<sup>9</sup>R. A. Baragiola, D. Chivers, D. Dodds, W. A. Grant, and J. S. Williams, Phys. Rev. Lett. A 56, 371 (1976); W. A. Grant, D. Dodds, J. S. Williams, C. E. Christodoulides, R. A. Baragiola, and D. Chivers, in Proceedings of the Fifth International Conference on Ion Implantation, August 1976, Boulder, Colorado (unpublished).

<sup>10</sup>M. M. Jakas and Don E. Harrison, Jr., Phys. Rev. B 30, 3573 (1984).

<sup>11</sup>O. B. Firsov, J. Exptl. Theoret. Phys (USSR) 33, 696 (1957) [Sov. Phys.—JETP 6, 534 (1958)].

<sup>12</sup>J. Lindhard, V. Nielsen, M. Scharff, and P. V. Thomsen, K. Dan. Vidensk. Selsk. Mat. Fys. Medd. 33, 10 (1963).

<sup>13</sup>P. Sigmund, M. T. Matthies, and D. L. Phillips, Radiat. Eff. 11, 39 (1971).

<sup>14</sup>S. Kalbitzer and H. Oetzmann, Radiat. Eff. 13, 215 (1980).

<sup>15</sup>M. T. Robinson, Philos. Mag. 12, 741 (1965); 17, 639 (1969).

<sup>16</sup>K. B. Winterbon, Radiat. Eff. 13, 215 (1972).

<sup>17</sup>This seems to be the case for metallic targets. In insulators electronic displacements are known to cause atomic displacements.

<sup>18</sup>A distinction must be made between  $\eta_1$  as given by Eq. (22) and  $\eta$  defined as the total amount of energy deposited in electronic excitations, because  $\eta_1$  contains the energy deposited by the primary ion, but not that deposited by earlier generations of recoil atoms.

<sup>19</sup>P. Sigmund, Appl. Phys. Lett. 14, 114 (1969).

<sup>20</sup>P. Sigmund, Phys. Rev. 184, 383 (1969).

<sup>21</sup>D. E. Harrison, Jr., Radiat. Eff. 70, 1 (1983).

<sup>22</sup>J. P. Biersack and W. Eckstein, Appl. Phys. A34, 73 (1984).

<sup>23</sup>L. M. Kishinevsky, Izv. Akad. Nauk SSSR (Ser. Fiz.) 26, 1410 (1962) [Bull. Acad. Sci. USSR (Phys. Ser.) 26, 1433 (1962)].

<sup>24</sup>R. Blume, W. Eckstein, H. Verbeek, and K. Reichelt, Nucl. Instrum. Methods 194, 67 (1982).

<sup>25</sup>O. S. Oen and M. T. Robinson, Nucl. Instrum. Methods 132, 647 (1976) and Ref. 3.